Chemical Science

ROYAL SOCIETY OF CHEMISTRY

EDGE ARTICLE

View Article Online
View Journal | View Issue

Cite this: *Chem. Sci.*, 2024, **15**, 6853

All publication charges for this article have been paid for by the Royal Society of Chemistry

Received 19th January 2024
Accepted 4th April 2024

DOI: 10.1039/d4sc00437j

rsc.li/chemical-science

Accelerating protein aggregation and amyloid fibrillation for rapid inhibitor screening†

Jingjin Fan, Liwen Liang, Xiaoyu Zhou* and Zheng Ouyang*

The accumulation and deposition of amyloid fibrils, also known as amyloidosis, in tissues and organs of patients has been found to be linked to numerous devastating neurodegenerative diseases. The aggregation of proteins to form amyloid fibrils, however, is a slow pathogenic process, and is a major issue for the evaluation of the effectiveness of inhibitors in new drug discovery and screening. Here, we used microdroplet reaction technology to accelerate the amyloid fibrillation process, monitored the process to shed light on the fundamental mechanism of amyloid self-assembly, and demonstrated the value of the technology in the rapid screening of potential inhibitor drugs. Proteins in microdroplets accelerated to form fibrils in milliseconds, enabling an entire cycle of inhibitor screening for Aβ40 within 3 minutes. The technology would be of broad interest to drug discovery and therapeutic design to develop treatments for diseases associated with protein aggregation and fibrillation.

Introduction

Neurodegenerative diseases, such as those caused by the infectious varieties of prions, Alzheimer's disease, and Parkinson's disease, are believed to be closely related to the accumulation of proteins and the formation of amyloid fibrils due to the misfolding of the proteins.[1,2] These disorders, caused by self-association, aggregation, or conformational changes in proteins, are also called "conformational diseases".[3–6] A significant feature of these disorders is the long progression and an extended latency period. The incubation or development period of pathogenic proteins *in vivo* typically lasts decades, from the asymptomatic protein misfolding at the beginning to the exhibition of symptoms such as the degeneration of brain or nerve cells, decline of elaborative ability, and loss of daily-activity independence.[7–9] Notably, these disorders are permanent and incurable; however, many of them are treatable through early diagnostics and treatment of symptoms to delay the progression of the disorders.

Rapid screening of inhibitors that disrupt protein aggregation contributes to the discovery of methods for treating such diseases. In traditional ways, structure-based design has been used to create small molecule inhibitors that can stabilize the native structure of the proteins, thus preventing the conformational changes to form protein aggregates. Specifically, inhibitors are typically bound to amyloid proteins under pathological conditions *in vitro*, and screening of inhibitors is achieved by evaluating the aggregation patterns through dye-binding assays. Such a procedure typically requires a noticeably long time, ranging from several hours to several days or even longer.[10,11] This issue needs to be addressed for rapid screening of inhibitor drugs.

Recently, the acceleration of slow chemical and biological processes has been enabled in microdroplets,[12–14] where the reaction rates are significantly enhanced by two to six orders of magnitude compared with those in batch syntheses.[15] Microdroplet reaction technology involves conducting chemical or biological reactions within extremely small droplets of electrospray or related techniques, and these droplets are typically in the microliter or even the picolitre range. The acceleration effect in microdroplets could be attributed to factors such as the high specific surface area, the strong electric field strength on the surface of microdroplets, and the enhanced collision frequency between reagents.[16–18] This technology is widely used in real-time reaction monitoring, rapid material preparation, protein sequencing, and protein characterization.[19,20] The interfacial effect has been found to be critical for protein aggregation.[21,22] In this study, we accelerated the processes in microdroplets for amyloid-like proteins. The progression in different stages of amyloid fibrillation was monitored by controlling the spray conditions, including soft-landing distance (L_d), pH value, spray voltage, *etc.* The obtained amyloid fibrils in microdroplets were systematically characterized by analytical tools, including transmission electron microscopy (TEM), specific fluorescent dye thioflavin T (ThT) binding, circular dichroism (CD), and mass spectrometry (MS). We show the good versatility of this method for accelerating the fibrillation of different proteins and

State Key Laboratory of Precision Measurement Technology and Instruments, Department of Precision Instrument, Tsinghua University, Beijing 100084, China. E-mail: zhouyuzxy@mail.tsinghua.edu.cn; ouyang@mail.tsinghua.edu.cn

† Electronic supplementary information (ESI) available: The experimental section, including details about chemicals, microdroplet generator capillary, fluorescence imaging, circular dichroism, transmission electron microscopy, and mass spectrometry analysis. See DOI: https://doi.org/10.1039/d4sc00437j

peptides and demonstrate the feasibility for rapid screening of fibrillar inhibitors.

Results and discussion

Accelerated fibril growth in microdroplets

Protein aggregation is a continuous self-assembly process consisting of multiple stages, as shown in Fig. 1a. Incorrect hydrophobic and hydrophilic interactions initiate the off pathway folding intermediates from the native proteins. Driven by intermolecular interactions, the intermediates further grow into β-sheet-rich aggregates or other not clearly defined secondary-structure oligomers.[23,24] These oligomers continue to interact and assemble into protofibrils with ordered fibrillar structures. Ultimately, matured, polymorphic, multi-chain amyloid-like fibrils are formed.

We chose a very common globular protein, myoglobin, to demonstrate the ability of microdroplet acceleration for protein aggregation at mildly alkaline pH values.[25–28] We prepared protein aggregates under alkaline conditions, other than physiological conditions, because of the following considerations. Alkaline conditions have been observed to facilitate the aggregation process more rapidly and efficiently compared to the process that would occur under physiological conditions.[25,26] This is a very effective evaluation of the judgment of fibril response. And alkaline conditions were commonly used as experimental conditions for protein fibrillation.[27,28] Moreover, it's well-documented that inflammation or chronic diseases can induce significant variations in the pH environment within biological systems. These pH fluctuations can profoundly affect the behaviour and stability of proteins. A plume of aqueous microdroplets containing 1 μg μL^{-1} globular myoglobin in ammonium acetate solution (pH adjusted to 9) was produced by a high voltage (4 kV) in a nano-electrospray ionization tip (Fig. 1b), and a detailed description could be found in the "Microdroplet generation module" within the ESI.† The protein aggregation reaction occurred in sprayed microdroplets and the fibril products were collected from a landing target plate. The reaction time was adjusted by varying the landing distance (L_d). The statistical results of fibril growth are shown in Fig. 1c and S1.† The representative transmission electron microscope (TEM) images in Fig. 1d reveal the synthesis of myoglobin fibrils at different landing distances L_d (0–30 mm). Exposure time and intensity of the e-beam for TEM imaging were adjusted to a suitable dose to avoid misjudgment. The estimated time was calculated by integrating the velocity of microdroplets over the landing distance, as in previous reports.[29–31] The measured velocity of microdroplets is about 1.35 m s^{-1} (ref. 32) (indicating a reaction time R_t of 22 ms for a L_d of 30 mm). We observed the formation of oligomers (100–200 nm) within 7 ms (corresponding to L_d = 10 mm, Fig. 1d and S1†). The oligomers further grew with the increment in the spray distance, *i.e.*, reaction time. For L_d = 30 mm, the maximum length of the fibrils grown in microdroplets was about 2 μm. The circular dichroism results (Fig. S2 and Table S1†) show the significant increase in β-sheets during the fibril formation in the traditional way. As a comparison, myoglobin aggregation in 50 mM sodium borate, pH 9.0 at 65 °C is shown in Fig. 1e–g and S3.† The results here indicated that the formation of amyloid fibrils in microdroplets was 10^6 times faster than that in traditional bulk reactions.

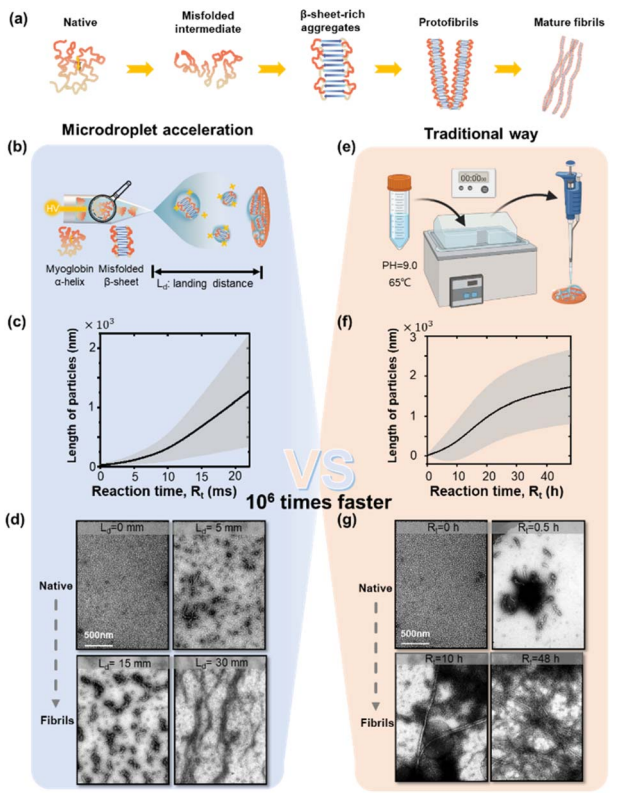

Fig. 1 Rapid fibril synthesis in microdroplets. (a) Schematic of the formation process of fibrillar aggregates. Performance comparison of protein aggregations between (b–d) microdroplet acceleration and (e–g) traditional methods. (b and e) Schematic of experimental workflows. (c and f) Length of the formed fibril as a function of the reaction time R_t. Reaction in microdroplets was 10^6 times faster than that using the traditional method. The error bars represent one standard deviation (SD) with 4 replicates. (d and g) TEM images of the fibrillation process. In microdroplet reactions, a landing distance, L_d, of 30 mm corresponds to a reaction time, R_t, of 22 ms. The scale bar is 500 nm.

Despite the widespread use of electrospray in the study of protein aggregation and amyloid fibrillation,[33–35] we showed that the reaction conditions in microdroplets, such as the pH value and ionization voltage, were crucial for the acceleration effect of fibril growth in microdroplets (Fig. S4 and S5†). The pH value is closely related to the initial structure, the electrostatic charges, and various interaction types of the protein. Myoglobin's isoelectric point (pI) falls within the range of 6.5 to 7.0. According to a previous report,[25,36] some amyloid-like fibril formation, such as myoglobin and human lysozyme, are prone to be induced under alkaline conditions. The results in Fig. S4† indicated that at slightly lower pH values near the pI, a pattern of particles with partial structural unfolding was observed, and these particles had smaller average sizes. As the pH value increases, the average length of the particles also increases, which confirms the pH-dependent acceleration of the

fibrillation reaction. Additionally, the pH changes during spraying are also non-negligible, which has been proven clearly in previous research.[37] The pH of a basic solution should increase as the volume decreases, and the basic species become more concentrated due to solvent evaporation which can further promote the occurrence of the reaction.[38] However, considering that ammonium acetate was used as the buffer solution, H^+ ions are generated by deprotonation of NH_4^+, thereby generating a buffer around the pK_a of ammonium,[39] and the effect of this evaporation mechanism on pH may be weakened in the case here. The ionization voltage is also a crucial factor influencing the rate of microdroplet reactions. Previous studies[40,41] have explored the electric field distribution at the microdroplet interface and found that, compared to the electric field formed by randomly arranged water molecules in the solution phase, the electric field generated by free O–H radicals on the droplet surface can reach approximately 16 mV cm^{-1}.[42] This electric field is sufficient to disrupt chemical bonds within the droplet, thereby driving more intense chemical reactions. When varying the spray voltage, it was observed that higher spray voltages were conducive to the generation of amyloid-like fibrils (Fig. S5†).

Characterization of the fibrils formed in microdroplets

We used multiple analytical tools for the confirmation of formation of fibrils in microdroplets. We analyzed the proteins and their aggregates before and after microdroplet accelerations in bulk solution (Fig. 2a, c, e) and electrified microdroplets (Fig. 2b, d, f), respectively. A shown in the TEM images, the protein particles showed no fibrillar aggregates under negative stain in the bulk phase even on applying a high voltage (4 kV) (Fig. 2a, left). However, upon the generation of microdroplets *via* high voltage (4 kV), protein particles revealed distinct fibrillar aggregates in TEM images (Fig. 2b, left).

To further confirm the formation of fibrils, protein particles in microdroplets after soft landing were stained by thioflavin T (ThT),[43,44] incubated for 1 hour, and detected by using a laser scanning confocal microscope. Using a 445 nm laser for excitation, a pronounced filamentous fluorescence signal was observed near the 482 nm range (Fig. 2b, right), while the regions without amyloid-like fibrils showed no significant signal at 482 nm (as shown in the control group in Fig. 2a, right). The redshift of ThT fluorescence dye indicated the presence of fibrillar β-sheet structures within the structure, confirming the occurrence of amyloid-like fibrillation reactions in microdroplets. Fluorescence emission spectra were shown in comparison with Fig. 2c and d.

CD analysis was also conducted and showed that the α-helices of myoglobin in the bulk phase (Fig. 2e) unfolded to form fibrillation structures or β-sheets in the microdroplets (Fig. 2f). The quantitative results of estimating secondary structure content from CD spectra for different states during spray are presented in Table S2.† The circular dichroism results indicated more than 80% reduction in α-helix content after acceleration *via* microdroplet reactions, while the β-sheet content increased 50-fold compared to that in the bulk phase.

The mass spectra of myoglobin in positive ion mode are also favorable evidence for the protein aggregations in microdroplets. As shown in Fig. S6,† broader envelopes were observed both at +8/+9 charge state distribution and in the high-mass range, suggesting the presence of inadequately desolvated aggregations, compared with those in bulk solution. The detail MS parameters could be found in Table S3.†

In the early stages of drug development, the primary focus lies in comprehending the behaviours of associated proteins before and after the disease, enabling the study of differential effects of various drug interventions.[27,45] β-Amyloids fibrils are proved to be intimately involved in the pathology of chronic neurodegenerative disease.[46] Thus, we use confocal laser microscopy, TEM, CD and mass spectrometry for the joint analysis which have proven that the fibrils prepared through microdroplets exhibit a high degree of structural consistency with naturally generated fibrils in both their initial and final states. The processes of protein fibrillation accelerated by microdroplets and under physiological conditions are comparable, which indicates that microdroplet technology is suitable for rapid drug discovery and screenings.

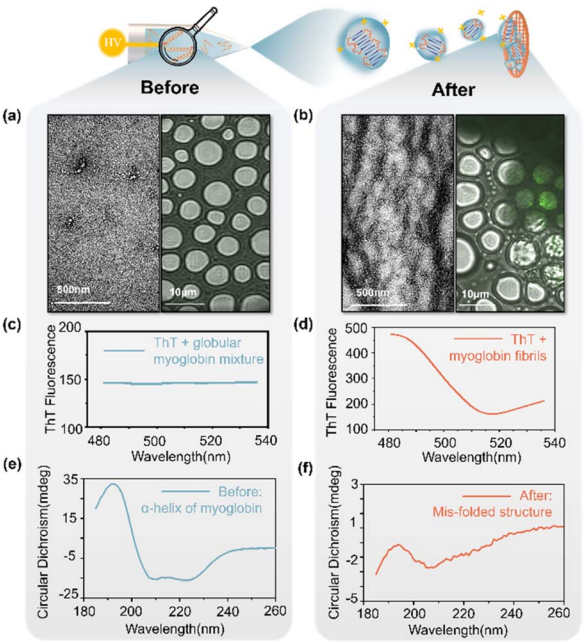

Fig. 2 Characterization of myoglobin amyloid-like aggregation in microdroplets before (a, c, and e in bulk solution on applying a high voltage) and after (b, d, and f in microdroplets) nano-electrospray (50 mM ammonium acetate, pH = 9); (a and b left) TEM, (a and b right) laser confocal fluorescence, (c and d) fluorescence emission spectra and (e and f) circular dichroism. The scale bars are 500 nm in TEM and 10 μm in laser confocal fluorescence.

Rapid fibrillation of Aβ and α-synuclein

Alzheimer's disease (AD) is the most common neurodegenerative disorder closely associated with the aggregation of β-amyloid (Aβ) within the brain. These specific assemblies of aggregated proteins are typically composed of residues, known

as β-amyloid peptides (Aβ-s), with Aβ40 and Aβ42 being the most common variant segments.[47–49] α-Synuclein has been postulated to play a central role in the pathogenesis of several neurodegenerative disorders. For example, the abnormal accumulation and aggregation of α-synuclein have been observed to be associated with the dysfunctionality and degeneration of neurons in Parkinson's disease (PD).[50] Here, aggregation kinetics of α-synuclein and β-amyloid proteins were explored.

Mass spectra of Aβ40, Aβ42 and α-synuclein are shown in Fig. 3, where the dimers, trimers, and tetramers of Aβ40 and Aβ42, and dimers of α-synuclein were labelled. TEM images of the proteins after the microdroplet reaction revealed the pronounced fibrillar aggregates at pH = 9, with size distributions ranging from 100 nm to 300 nm for Aβ40 and α-synuclein, up to 600 nm for Aβ42 (insets, Fig. 3a–c and S8–S10†).

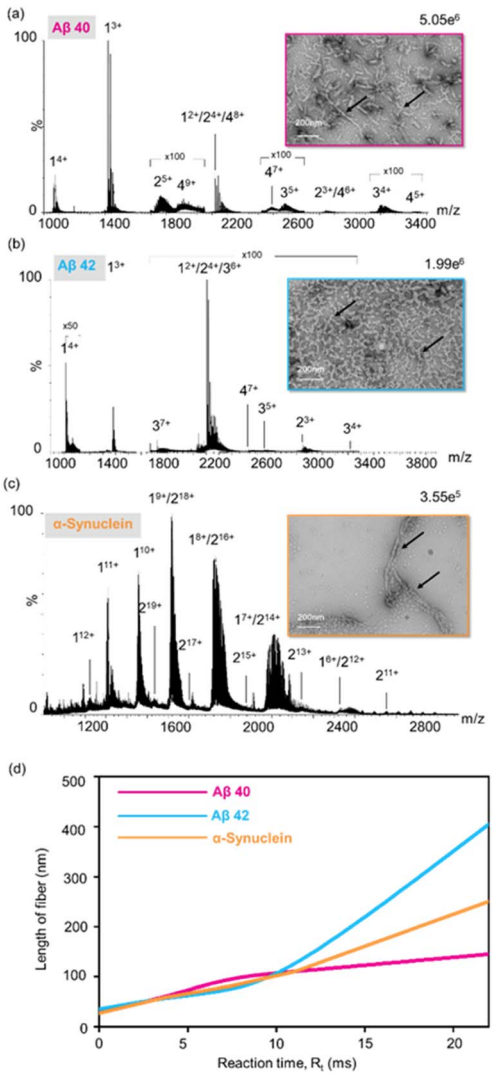

Fig. 3 Characterization of the amyloid-like aggregation of peptides associated with clinical amyloidosis in the microdroplet reaction. Mass spectra of (a) Aβ40 (b) Aβ42 and (c) α-synuclein and their oligomers. Inset shows TEM images of the aggregates. The scale bar is 200 nm. (d) Synthesis rate in microdroplets: R_t-course change in the length of protein particles.

Nevertheless, in the control group at pH = 7, only monomers were observed in the mass spectra and no fibrils were observed in TEM images (Fig. S7†). Fig. 3d shows the synthesis rates in microdroplets. Furthermore, through varying the landing distance, L_d, the progress of protein fibrillation within microdroplets was controlled. As L_d increased from 0 mm to 30 mm, the average length of particles in the field of view steadily increased correspondingly (Fig. S8–S10†).

Rapid inhibitor screening

The screening of inhibitor drugs is crucial for neurodegenerative diseases caused by fibrillation.[51] A dual-head nanoelectrospray ion source, one containing Aβ40 solution and the other containing small molecule inhibitor solution, was used to produce reactant microdroplets. The spatial position of the mesh was controlled by using a three-dimensional movement platform with an internally designed *x*–*y*–*z* three-dimensional movement system, and the two capillaries were symmetrically positioned with an included angle ranging from 60° to 70°. When only with Aβ protein, under suitable microdroplet acceleration reaction conditions, it will undergo the nucleation aggregation. However, the introduction of microdroplets containing inhibitors hinders the nucleation aggregation process. A schematic diagram of the instrumentation setup and reaction mechanism is illustrated in Fig. S11.†

Screening of small molecular drugs[52–54] was demonstrated in the following section. Here, epigallocatechin gallate (EGCG), tramiprosate, quercetin, furosemide, and 3-ethoxysalicylaldehyde have been illustrated to inhibit the fibrillation of Aβ40, while hemin cannot. Hemin is effective for kappa-casein, lysozyme amyloidosis and αSyn, but not for Aβ40. Setting the concentration ratio of Aβ40 and EGCG to 1 : 20,[55,56] microdroplet reactions were conducted using the mentioned method. Comparing with the TEM results in Fig. 4a, it was evident that Aβ40 aggregation was significantly inhibited with EGCG. Previous research has also shown that tramiprosate can delay *in vivo* fibril synthesis by binding to soluble Aβ40. The experimental group with the tramiprosate inhibitor exhibited a noticeable reduction in the distribution of fibrils at around 200 nm. Quercetin has shown that H-bond interaction between the OH group and Aβ fibril leads to the formation of modified oligomers and hinders the creation of β-sheet structures,[57,58] furosemide exhibits Aβ-oligomerization-inhibiting activity *in vitro*,[59] and 3-ethoxysalicylaldehyde interferes with hydrophobic and/or pi–pi interactions and thus prevents the self-association of Aβ.[60] In the experimental group with these five inhibitors, significant aggregation inhibition was observed. As for another small molecule, hemin, no impact on Aβ40 protein self-assembly was observed, suggesting that it cannot bind to Aβ40 to disturb the formation of fibrils.

Statistical analysis of the interactions between the three small molecules and Aβ40 is shown in Fig. 4b. As expected, EGCG, tramiprosate, quercetin, furosemide, and 3-ethoxysalicylaldehyde had a significant inhibitory effect on fibril growth, effectively reducing the aggregation formation of Aβ40 with different effects. However, hemin didn't show a significant

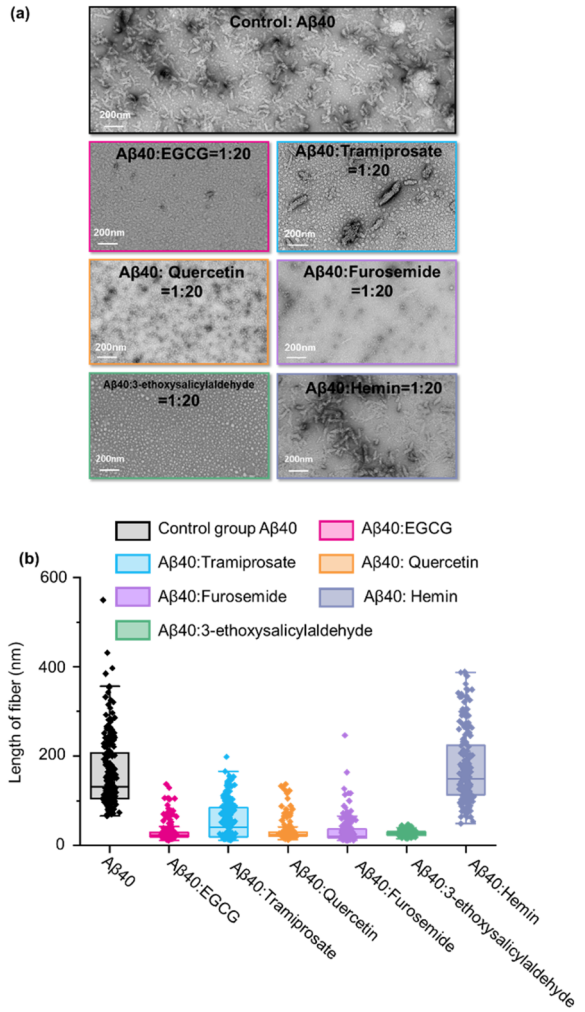

Fig. 4 Statistical differences in binding Aβ40 with small molecule drugs. TEM images of fibrillar aggregation of Aβ40 in microdroplets with (a) no inhibitor applied (black line); inhibitor EGCG, tramiprosate, quercetin, furosemide, and 3-ethoxysalicylaldehyde; and negative control hemin. The concentration ratios of Aβ40 and small molecules were all 1 : 20. (b) Statistical representation of fibrillation lengths in TEM images. The central line in the box plot represents the median of the samples.

contribution to the disaggregation of Aβ40. The screening results in microdroplets here matched with the previous report[53] and those performed in the conventional way in bulk solution (Fig. S12†), demonstrating the application potential of the technology for rapid inhibitor drug discovery and distinguishing the inhibitors *via* the different effects and functional mechanisms. An entire cycle of inhibitor screening for Aβ40 was within 3 minutes, including microdroplet reaction, product collection, and TEM and MS evaluations. This is a significant improvement of the efficiency for rapid screening of inhibitors.

Conclusions

In conclusion, a microdroplet acceleration method was developed to expedite the formation of protein amyloid fibrils. The accelerated synthesis of amyloid-like fibrils in microdroplets was confirmed through comprehensive validation approaches, encompassing different structural biology tools. In the showcased examples, the protein and peptide associated with clinical amyloidosis exhibited potential for fibril formation, and the fibrillation processes were accelerated by approximately six orders of magnitude. As the first demonstration of fibrillation acceleration in microdroplets, the technology showed potential in applications such as synthesis of oligomer amyloids and inhibitor screening for treatment of neurodegenerative diseases.

Data availability

The data underlying this study are available in the published article and its ESI.†

Author contributions

J. F., X. Z., and Z. O. conceived the research and co-wrote the manuscript. X. Z. and Z. O. provided funding support for the research. J. F. and L. L. designed and performed all the experiments and conducted all the data analysis. X. Z. and Z. O. supervised the research. All authors discussed the results and supported the manuscript writing.

Conflicts of interest

There are no conflicts to declare.

Acknowledgements

This work was supported by the National Natural Science Foundation of China (Project No. 22374088, 22227807, and 21934003)

Notes and references

1 M. P. Rout and A. Sali, Principles for integrative structural biology studies, *Cell*, 2019, **177**, 1384–1403.
2 D. J. Selkoe, Folding proteins in fatal ways, *Nature*, 2003, **426**, 900–904.
3 R. W. Carrell and D. A. Lomas, Conformational disease, *Lancet*, 1997, **350**, 134–138.
4 T. P. Knowles, M. Vendruscolo and C. M. Dobson, The amyloid state and its association with protein misfolding diseases, *Nat. Rev. Mol. Cell Biol.*, 2014, **15**, 384–396.
5 D. Li and C. Liu, Conformational strains of pathogenic amyloid proteins in neurodegenerative diseases, *Nat. Rev. Neurosci.*, 2022, **23**, 523–534.
6 R. R. Kopito and D. Ron, Conformational disease, *Nat. Cell Biol.*, 2000, **2**, E207–E209.
7 J. Collinge, J. Whitfield, E. McKintosh, J. Beck, S. Mead, D. J. Thomas and M. P. Alpers, Kuru in the 21st century—an acquired human prion disease with very long incubation periods, *Lancet*, 2006, **367**, 2068–2074.

8 Z. Jaunmuktane, G. Banerjee, S. Paine, A. Parry-Jones, P. Rudge, J. Grieve, A. K. Toma, S. F. Farmer, S. Mead and H. Houlden, Alzheimer's disease neuropathological change three decades after iatrogenic amyloid-β transmission, *Acta Neuropathol.*, 2021, **142**, 211–215.
9 C. Duyckaerts, F. Clavaguera and M.-C. Potier, The prion-like propagation hypothesis in Alzheimer's and Parkinson's disease, *Curr. Opin. Neurobiol.*, 2019, **32**, 266–271.
10 S. K. Palaninathan, N. N. Mohamedmohaideen, W. C. Snee, J. W. Kelly and J. C. Sacchettini, Structural insight into pH-induced conformational changes within the native human transthyretin tetramer, *J. Mol. Biol.*, 2008, **382**, 1157–1167.
11 T. Scheibel and S. L. Lindquist, The role of conformational flexibility in prion propagation and maintenance for Sup35p, *Nat. Struct. Mol. Biol.*, 2001, **8**, 958–962.
12 Z. Wei, Y. Li, R. G. Cooks and X. Yan, Accelerated reaction kinetics in microdroplets: overview and recent developments, *Annu. Rev. Phys. Chem.*, 2020, **71**, 31–51.
13 Y. Li, X. Yan and R. G. Cooks, The role of the interface in thin film and droplet accelerated reactions studied by competitive substituent effects, *Angew. Chem., Int. Ed.*, 2016, **55**, 3433–3437.
14 I. Nam, J. K. Lee, H. G. Nam and R. N. Zare, Abiotic production of sugar phosphates and uridine ribonucleoside in aqueous microdroplets, *Proc. Natl. Acad. Sci. U. S. A.*, 2017, **114**, 12396–12400.
15 J. K. Lee, D. Samanta, H. G. Nam and R. N. Zare, Spontaneous formation of gold nanostructures in aqueous microdroplets, *Nat. Commun.*, 2018, **9**, 1562.
16 J. K. Lee, S. Banerjee, H. G. Nam and R. N. Zare, Acceleration of reaction in charged microdroplets, *Q. Rev. Biophys.*, 2015, **48**, 437–444.
17 S. Banerjee, E. Gnanamani, X. Yan and R. N. Zare, Can all bulk-phase reactions be accelerated in microdroplets?, *Analyst*, 2017, **142**, 1399–1402.
18 C. J. Chen and E. R. Williams, The role of analyte concentration in accelerated reaction rates in evaporating droplets, *Chem. Sci.*, 2023, **14**, 4704–4713.
19 X. Zhong, H. Chen and R. N. Zare, Ultrafast enzymatic digestion of proteins by microdroplet mass spectrometry, *Nat. Commun.*, 2020, **11**, 1049.
20 X. Yan, R. M. Bain and R. G. Cooks, Organic reactions in microdroplets: reaction acceleration revealed by mass spectrometry, *Angew. Chem., Int. Ed.*, 2016, **55**, 12960–12972.
21 S. Campioni, G. Carret, S. Jordens, L. c. Nicoud, R. Mezzenga and R. Riek, The presence of an air–water interface affects formation and elongation of α-synuclein fibrils, *J. Am. Chem. Soc.*, 2014, **136**, 2866–2875.
22 S. Jordens, L. Isa, I. Usov and R. Mezzenga, Non-equilibrium nature of two-dimensional isotropic and nematic coexistence in amyloid fibrils at liquid interfaces, *Nat. Commun.*, 2013, **4**, 1917.
23 Y. Sun, A. Kakinen, Y. Xing, P. Faridi, A. Nandakumar, A. W. Purcell, T. P. Davis, P. C. Ke and F. Ding, Amyloid self-assembly of hIAPP8-20 *via* the accumulation of helical oligomers, α-helix to β-sheet transition, and formation of β-barrel intermediates, *Small*, 2019, **15**, 1805166.
24 F. Chiti and C. M. Dobson, Protein misfolding, functional amyloid, and human disease, *Annu. Rev. Biochem.*, 2006, **75**, 333–366.
25 M. Fändrich, M. A. Fletcher and C. M. Dobson, Amyloid fibrils from muscle myoglobin, *Nature*, 2001, **410**, 165–166.
26 A. F. Brunger, H. L. Nienhuis, J. Bijzet and B. P. Hazenberg, Causes of AA amyloidosis: a systematic review, *Amyloid*, 2020, **27**, 1–12.
27 A. K. Buell, C. Galvagnion, R. Gaspar, E. Sparr, M. Vendruscolo, T. P. Knowles, S. Linse and C. M. Dobson, Solution conditions determine the relative importance of nucleation and growth processes in α-synuclein aggregation, *Proc. Natl. Acad. Sci. U. S. A.*, 2014, **111**, 7671–7676.
28 Y. Tian and J. H. Viles, pH Dependence of Amyloid-β Fibril Assembly Kinetics: Unravelling the Microscopic Molecular Processes, *Angew. Chem., Int. Ed.*, 2022, **61**, e202210675.
29 J. K. Lee, S. Kim, H. G. Nam and R. N. Zare, Microdroplet fusion mass spectrometry for fast reaction kinetics, *Proc. Natl. Acad. Sci. U. S. A.*, 2015, **112**, 3898–3903.
30 P. Kebarle and U. H. Verkerk, Electrospray: from ions in solution to ions in the gas phase, what we know now, *Mass Spectrom. Rev.*, 2009, **28**, 898–917.
31 A. Venter, P. E. Sojka and R. G. Cooks, Droplet dynamics and ionization mechanisms in desorption electrospray ionization mass spectrometry, *Anal. Chem.*, 2006, **78**, 8549–8555.
32 E. T. Jansson, Y.-H. Lai, J. G. Santiago and R. N. Zare, Rapid hydrogen–deuterium exchange in liquid droplets, *J. Am. Chem. Soc.*, 2017, **139**, 6851–6854.
33 S. L. Bernstein, N. F. Dupuis, N. D. Lazo, T. Wyttenbach, M. M. Condron, G. Bitan, D. B. Teplow, J.-E. Shea, B. T. Ruotolo and C. V. Robinson, Amyloid-β protein oligomerization and the importance of tetramers and dodecamers in the aetiology of Alzheimer's disease, *Nat. Chem.*, 2009, **1**, 326–331.
34 G. Li, K. DeLaney and L. Li, Molecular basis for chirality-regulated Aβ self-assembly and receptor recognition revealed by ion mobility-mass spectrometry, *Nat. Commun.*, 2019, **10**, 5038.
35 C. A. Scarff, A. E. Ashcroft and S. E. Radford, *Protein amyloid aggregation*, Springer, 2016.
36 D. Canet, A. M. Last, P. Tito, M. Sunde, A. Spencer, D. B. Archer, C. Redfield, C. V. Robinson and C. M. Dobson, Local cooperativity in the unfolding of an amyloidogenic variant of human lysozyme, *Nat. Struct. Biol.*, 2002, **9**, 308–315.
37 L. Konermann, Z. Liu, Y. Haidar, M. J. Willans and N. A. Bainbridge, On the Chemistry of Aqueous Ammonium Acetate Droplets during Native Electrospray Ionization Mass Spectrometry, *Anal. Chem.*, 2023, **95**, 13957–13966.
38 M. Girod, X. Dagany, R. Antoine and P. Dugourd, Relation between charge state distributions of peptide anions and pH changes in the electrospray plume. A mass spectrometry and optical spectroscopy investigation, *Int. J. Mass Spectrom.*, 2011, **308**, 41–48.

39 L. Konermann, Addressing a common misconception: ammonium acetate as neutral pH "buffer" for native electrospray mass spectrometry, *J. Am. Soc. Mass Spectrom.*, 2017, **28**, 1827–1835.
40 C. Gong, D. Li, X. Li, D. Zhang, D. Xing, L. Zhao, X. Yuan and X. Zhang, Spontaneous reduction-induced degradation of viologen compounds in water microdroplets and its inhibition by host–guest complexation, *J. Am. Chem. Soc.*, 2022, **144**, 3510–3516.
41 L. Zhao, X. Song, C. Gong, D. Zhang, R. Wang, R. N. Zare and X. Zhang, Sprayed water microdroplets containing dissolved pyridine spontaneously generate pyridyl anions, *Proc. Natl. Acad. Sci. U. S. A.*, 2022, **119**, e2200991119.
42 H. Hao, I. Leven and T. Head-Gordon, Can electric fields drive chemistry for an aqueous microdroplet?, *Nat. Commun.*, 2022, **13**, 280.
43 L. S. Wolfe, M. F. Calabrese, A. Nath, D. V. Blaho, A. D. Miranker and Y. Xiong, Protein-induced photophysical changes to the amyloid indicator dye thioflavin T, *Proc. Natl. Acad. Sci. U. S. A.*, 2010, **107**, 16863–16868.
44 P. S. Vassar and C. F. Culling, Fluorescent stains, with special reference to amyloid and connective tissues, *Arch. Pathol.*, 1959, **68**, 487–498.
45 W. P. Esler, E. R. Stimson, J. R. Ghilardi, A. M. Felix, Y.-A. Lu, H. V. Vinters, P. W. Mantyh and J. E. Maggio, Aβ deposition inhibitor screen using synthetic amyloid, *Nat. Biotechnol.*, 1997, **15**, 258–263.
46 R. Frank and R. Hargreaves, Clinical biomarkers in drug discovery and development, *Nat. Rev. Drug Discovery*, 2003, **2**, 566–580.
47 M. Schmidt, C. Sachse, W. Richter, C. Xu, M. Fändrich and N. Grigorieff, Comparison of Alzheimer Aβ (1–40) and Aβ (1–42) amyloid fibrils reveals similar protofilament structures, *Proc. Natl. Acad. Sci. U. S. A.*, 2009, **106**, 19813–19818.
48 D. B. Teplow, N. D. Lazo, G. Bitan, S. Bernstein, T. Wyttenbach, M. T. Bowers, A. Baumketner, J.-E. Shea, B. Urbanc and L. Cruz, Elucidating amyloid β-protein folding and assembly: a multidisciplinary approach, *Acc. Chem. Res.*, 2006, **39**, 635–645.
49 M. Verdurand, F. Chauveau, A. Daoust, A.-L. Morel, F. Bonnefoi, F. Liger, A. Bérod and L. Zimmer, Differential effects of amyloid-beta 1–40 and 1–42 fibrils on 5-HT1A serotonin receptors in rat brain, *Neurobiol. Aging*, 2016, **40**, 11–21.
50 M. Sharma and J. Burré, α-Synuclein in synaptic function and dysfunction, *Trends Neurosci.*, 2023, **46**, 153–166.
51 Y. R. Butler, Y. Liu, R. Kumbhar, P. Zhao, K. Gadhave, N. Wang, Y. Li, X. Mao and W. Wang, α-Synuclein fibril-specific nanobody reduces prion-like α-synuclein spreading in mice, *Nat. Commun.*, 2022, **13**, 4060.
52 S. Sonavane, S. Z. Haider, A. Kumar and B. Ahmad, Hemin is able to disaggregate lysozyme amyloid fibrils into monomers, *Biochim. Biophys. Acta, Proteins Proteomics*, 2017, **1865**, 1315–1325.
53 L. M. Young, J. C. Saunders, R. A. Mahood, C. H. Revill, R. J. Foster, L.-H. Tu, D. P. Raleigh, S. E. Radford and A. E. Ashcroft, Screening and classifying small-molecule inhibitors of amyloid formation using ion mobility spectrometry–mass spectrometry, *Nat. Chem.*, 2015, **7**, 73–81.
54 E. Y. Hayden, P. Kaur, T. L. Williams, H. Matsui, S.-R. Yeh and D. L. Rousseau, Heme stabilization of α-synuclein oligomers during amyloid fibril formation, *Biochemistry*, 2015, **54**, 4599–4610.
55 A. J. Doig and P. Derreumaux, Inhibition of protein aggregation and amyloid formation by small molecules, *Curr. Opin. Struct. Biol.*, 2015, **30**, 50–56.
56 S.-H. Wang, X.-Y. Dong and Y. Sun, Thermodynamic analysis of the molecular interactions between amyloid β-protein fragments and (−)-epigallocatechin-3-gallate, *J. Phys. Chem. B*, 2012, **116**, 5803–5809.
57 A. Alghamdi, D. J. Birch, V. Vyshemirsky and O. J. Rolinski, Impact of the Flavonoid Quercetin on β-Amyloid Aggregation Revealed by Intrinsic Fluorescence, *J. Phys. Chem. B*, 2022, **126**, 7229–7237.
58 A. Espargaró, T. Ginex, M. d. M. Vadell, M. A. Busquets, J. Estelrich, D. Muñoz-Torrero, F. J. Luque and R. Sabate, Combined *in vitro* cell-based/in silico screening of naturally occurring flavonoids and phenolic compounds as potential anti-Alzheimer drugs, *J. Nat. Prod.*, 2017, **80**, 278–289.
59 W. Zhao, J. Wang, L. Ho, K. Ono, D. B. Teplow and G. M. Pasinetti, Identification of antihypertensive drugs which inhibit amyloid-β protein oligomerization, *J. Alzheimer's Dis.*, 2009, **16**, 49–57.
60 F. G. De Felice, M. N. Vieira, L. M. Saraiva, J. D. Figueroa-Villar, J. Garcia-Abreu, R. Liu, L. Chang, W. L. Klein and S. T. Ferreira, Targeting the neurotoxic species in Alzheimer's disease: inhibitors of Aβ oligomerization, *FASEB J.*, 2004, **18**, 1366–1372.